Supplementary material for

SIV replication in the infected rhesus macaque is limited by the size of the pre-existing Th17 cell compartment

Dennis J. Hartigan-O'Connor, Kristina Abel, Koen K. A. Van Rompay, Bittoo Kanwar, and Joseph M. McCune

correspondence to: dhartigan@medsfgh.ucsf.edu

This PDF file includes:

Figure S1. Relationships between Th17 cells, T-regs, and memory T cells in uninfected macaques.
Figure S2. Infection parameters and immune cells in the observational study.
Figure S3. Effects of IL-2 and G-CSF on various immune cells.
Figure S4. Infection parameters and immune cells in the interventional study.
Figure S5. Relationship of T-regs to viral load and T cell activation.
Figure S6. Gating tree and typical raw data for the IL-17 and IFN-γ parameters.
Table S1. MHC alleles of animals in the observational study.

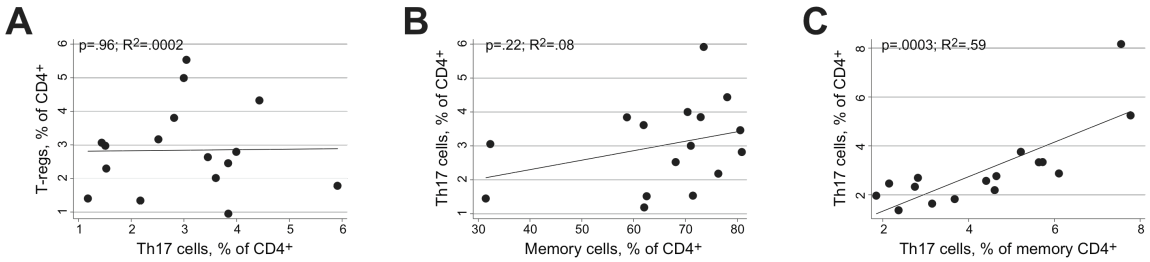

Figure S1. Relationships between Th17 cells, T-regs, and memory T cells in uninfected macaques.
(A) There was no consistent trend to an inverse relationship between the frequency of T-regs and Th17 cells. (B) Th17 cell frequency among all CD4+ T cells was not correlated with the frequency of CD4+ memory cells. (C) Th17 cell frequency was strongly correlated with Th17 cell frequency among memory CD4+ T cells.

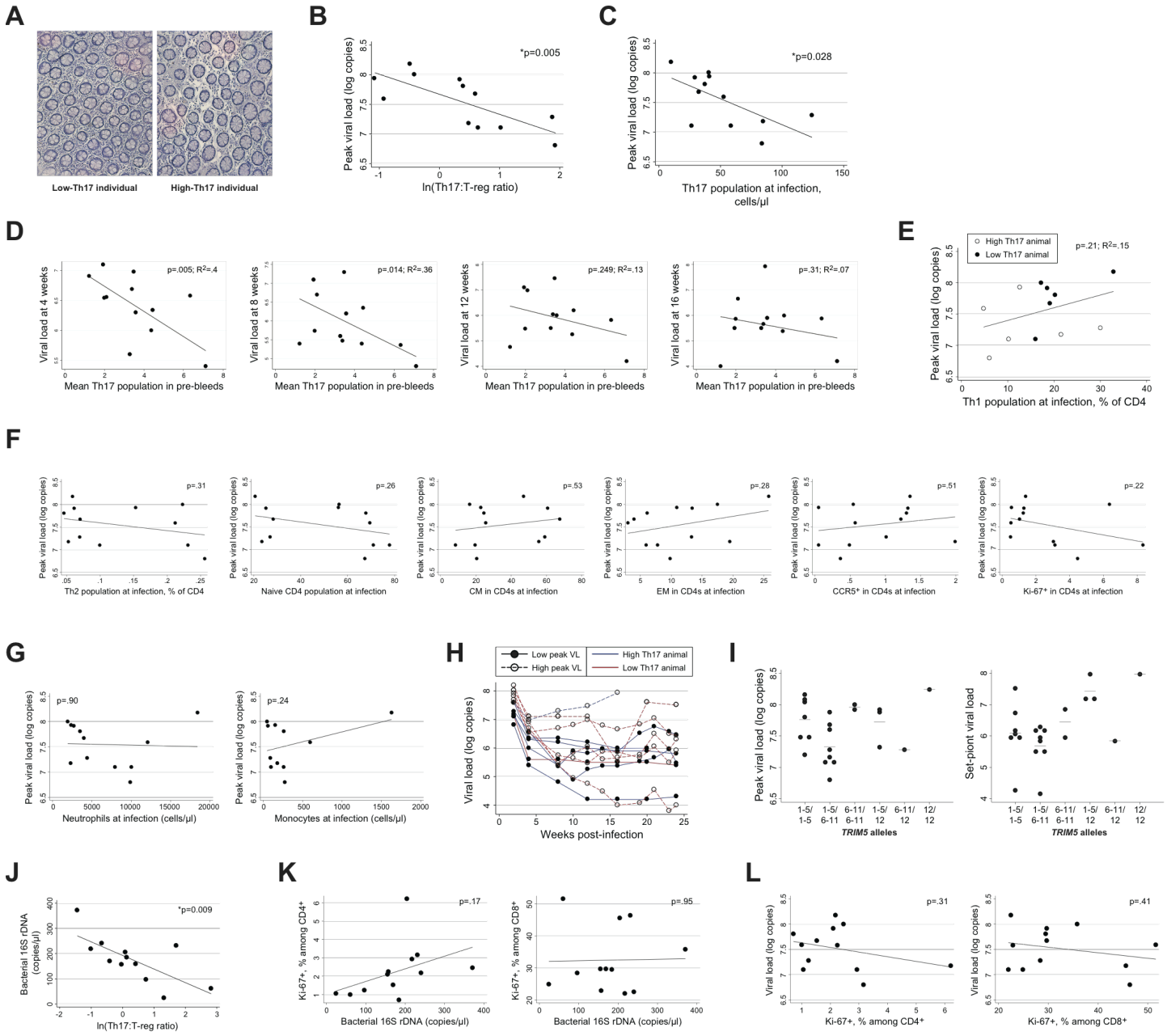

Figure S2. Infection parameters and immune cells in the observational study.
(A) Normal histological appearance of colon tissue from low-Th17 (left image) and high-Th17 (right image) individuals. DAB+ (brown) cells in these images are FoxP3+. (B) The correlation between the Th17:T-reg ratio and peak viral load is comparable to the correlation between the fractional Th17 cell population and peak viral load (Fig. 2A). (C) The absolute number of circulating Th17 cells present at infection is also predictive of peak viral load. (D) Relationship between the pre-infection level of Th17 cells and viral load degrades over time. From left to right, panels show viral loads at 4, 8, 12, and 16 weeks after infection. (E) The Th1 population present before infection was not predictive of viral loads. Individuals with pre-infection Th17 levels below the median are shown with closed markers; those with levels above the median are shown with open markers. (F) CD4+ T cell subsets demonstrating no consistent relationship with viral load included Th2 cells (expressing IL-4), naïve cells (CD45RA+CD27+), central memory cells (CD45RA-CD27+), effector memory cells (CD45RA-CD27-), CCR5+ cells, and Ki-67+ cells. (G) Numbers of circulating monocytes and neutrophils were also not predictive of viral load. (H) Animals with a high peak viral load (i.e., peak viral load above the median; shown with open circles and dashed lines) did not always experience a high set-point; animals with a low peak viral viral load (below the median; closed circles and solid lines) did not always experience a low set point. Individuals with pre-infection Th17 levels below the median are shown with red lines; those with levels above the median are shown with blue lines. (I) TRIM5 alleles were not predictive of peak or set-point viral loads (left and right panels, respectively). Allele numbering is from ref. 42. Alleles 1-5 only correspond to "low" intrinsic susceptibility to SIVmac251 infection, alleles 1-5 and 6-11 to "medium" susceptibility, and alleles 6-11 to "high" susceptibility (42). The influence of genotypes that include allele 12 has not been reported. The p values for differences in the median peak and set-point viral loads were non-significant (p=0.08 and 0.06 by Kruskal-Wallis test). (J) Bacterial 16S rDNA measured in plasma samples from infected animals is correlated with the Th17:T-reg ratio at two weeks after infection. (K) At 12 weeks after infection, there was no significant relationship between circulating bacterial 16S rDNA levels and generalized T cell activation, as assessed by Ki-67 expression in CD4+ and CD8+ T cells (left and right panels, respectively). (L) At 12 weeks after infection, CD4+ and CD8+ T cell activation were not correlated with viral load (left and right panels, respectively).

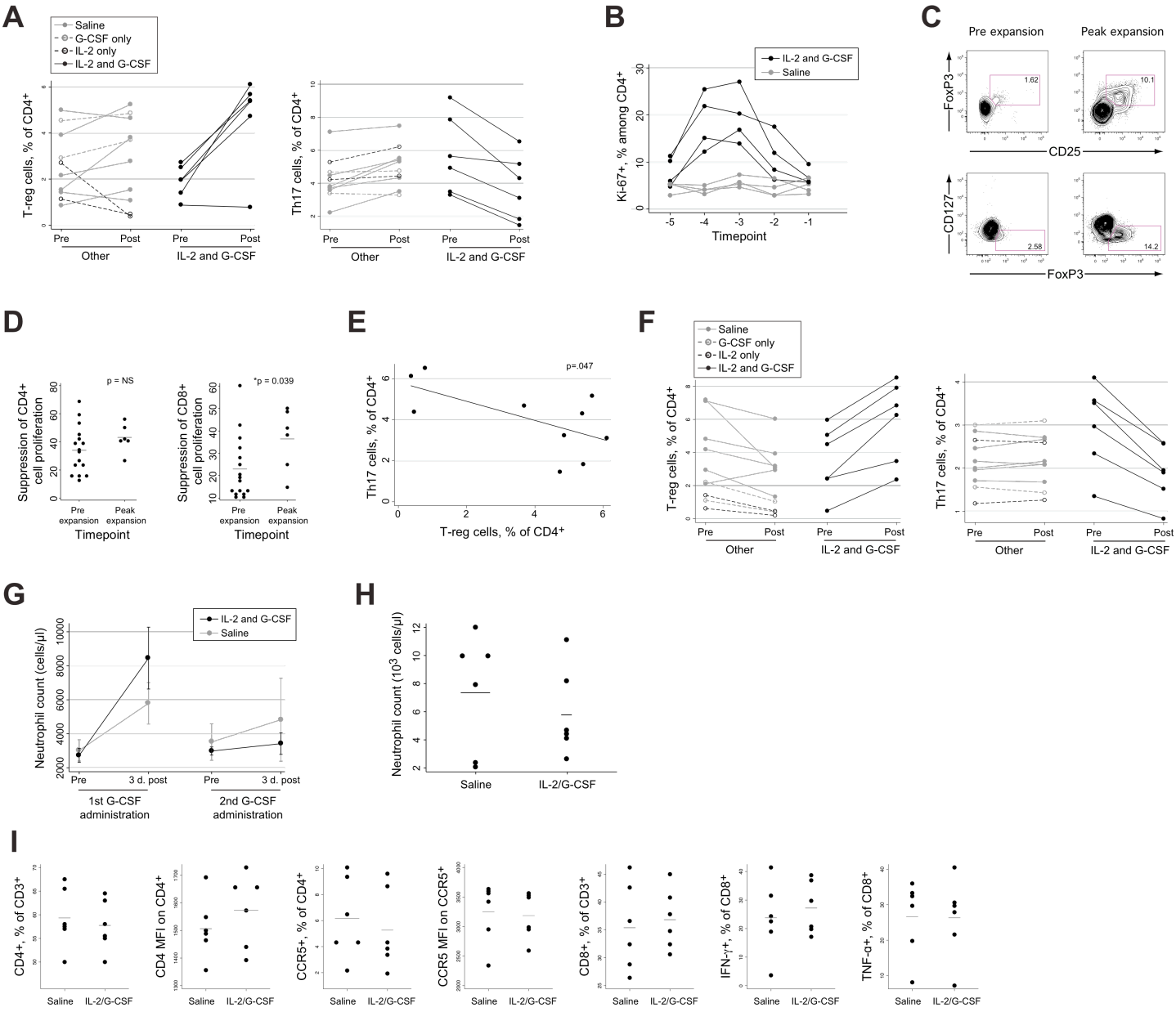

Figure S3. Effects of IL-2 and G-CSF on various immune cells.
(A) Treatment with IL-2 and G-CSF causes an increase in the fraction of T-regs and reduction in the fraction of Th17 cells among CD4+ T cells. Left panel shows the overall change in the percentage of T-reg cells found in CD4+ T cells between the start and the end of treatment. Right panel shows the overall change in the percentage of Th17 cells found in CD4+ T cells between the start and the end of treatment. (B) Treatment with IL-2 and G-CSF (black lines) causes a dramatic increase in Ki-67 expression in CD4+ T cells, indicating movement of cells into the cell cycle. (C) Expanded cells are FoxP3+ and CD127low. The FoxP3 expression observed in expanded cells is comparable to or greater than that observed before expansion. (D) Expanded cells have suppressive function that is comparable to or greater than that of unexpanded T-regs. In each panel, the left column ("Pre expansion") shows suppression demonstrated in the entire group of 16 animals before IL-2 and G-CSF treatment. The right column ("Peak expansion") shows suppression demonstrated in the six animals receiving IL-2 and G-CSF. T-regs were "added back" to CD25-depleted responder cells at a 1:3 ratio and suppression was calculated according to the formula in the Methods section. Thus, the ordinate shows the degree of suppression observed, with higher numbers indicating greater suppressive activity. The p values shown were calculated using the Mann-Whitney U test. (E) Treated animals developed an inverse relationship between T-regs and Th17 cells. (F) Treatment with IL-2 and G-CSF causes an increase in the fraction of T-regs and reduction in the fraction of Th17 cells among CD4+ T cells in lymph node tissue. Panels are arranged as in (A). (G) Change in neutrophil counts occurring with G-CSF treatment. The graph shows the absolute neutrophil count measured before and after the first or second administration of G-CSF (left and right, respectively). An increase was detectable three days after the first treatment but not three days after a second treatment. Data are mean +/- SE. (H) Neutrophil counts in saline-treated and IL-2/G-CSF-treated animals at the time of infection with SIV, three days after cessation of G-CSF. No difference in neutrophil counts is apparent. (I) Expression of cellular receptors used for viral entry as well as frequency and function of CD8+ T cells in treated and untreated groups. Each panel shows the percent positive or the MFI of the marker indicated on the vertical axis. In the last two panels, percent cytokine-expressing cells is shown after stimulation with PMA and ionomycin.

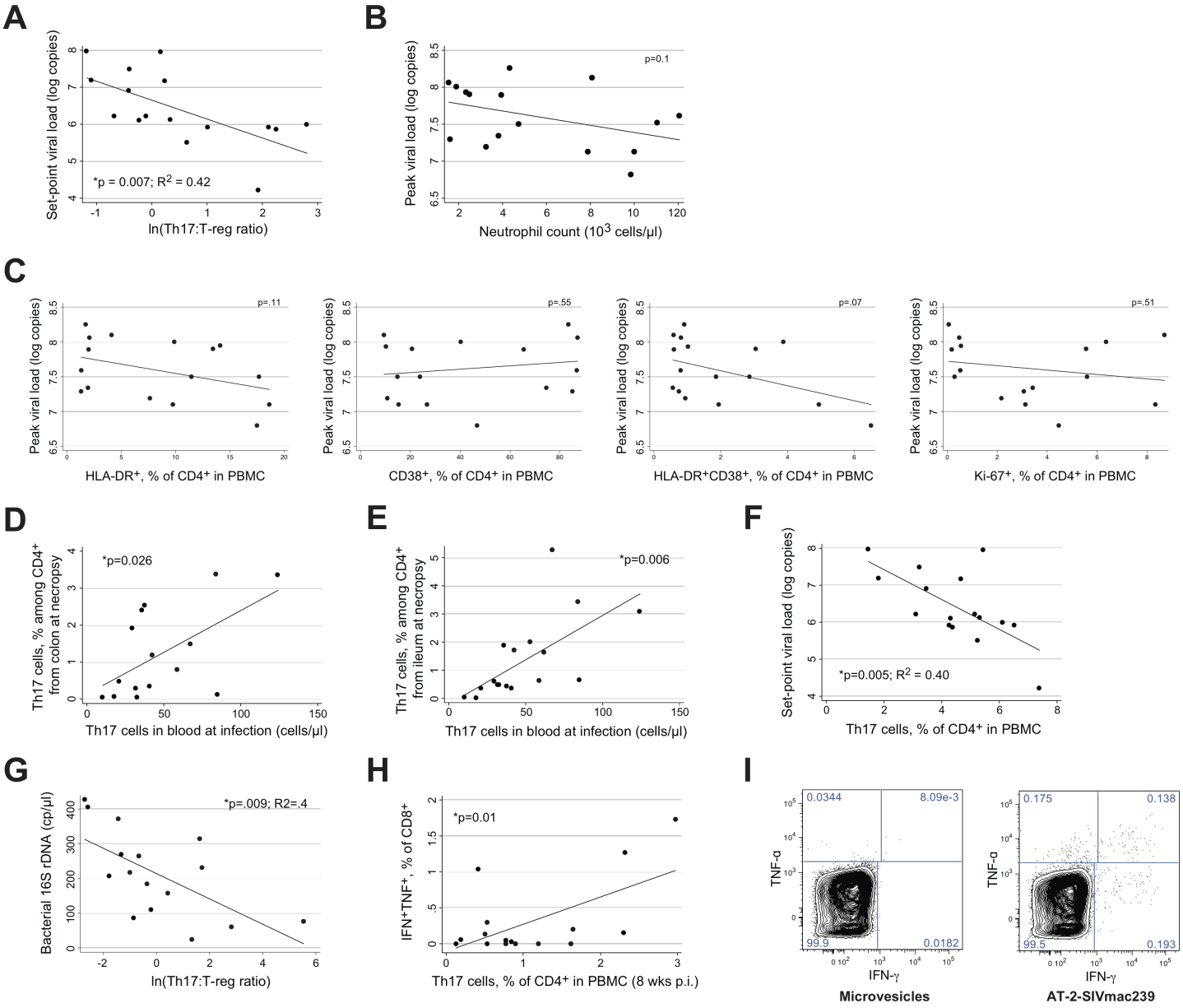

Figure S4. Infection parameters and immune cells in the interventional study.
(A) There is a significant relationship between Th17:T-reg ratios present on the day of infection and set-point viral loads established 3 to 6 months later. The set-point viral loads plotted here represent the geometric mean viral load at timepoints at or beyond the twelfth week of infection. (B) Relationship between neutrophil counts at the time of infection (abscissa) and peak viral loads (ordinate). The p value shown was calculated using linear regression. Addition of the fraction of Th17 cells or the Th17:T-reg ratio to this model also did not yield a significant result for the neutrophil term (p=0.47 or 0.16, respectively). (C) Measures of immune activation in CD4+ T cells (HLA-DR+, CD38+, HLA-DR+CD38+, or Ki-67+) were not predictive of increased viral loads. (D) The absolute number of Th17 cells in blood at the time of infection accurately predicts recovery of Th17 cells from colon tissue six months later. (E) The absolute number of Th17 cells in blood at the time of infection accurately predicts recovery of Th17 cells from ileal tissue six months later. (F) The fraction of Th17 cells present at infection is predictive of the set-point viral load that develops 3 to 6 months later. (G) Bacterial 16S rDNA levels in plasma, assessed by real-time PCR, are correlated with the log Th17:T-reg ratio at 2 weeks after infection. (H) Th17 cells (abscissa) and CD8+ T cell responses (ordinate) to p27 peptides are correlated eight weeks after infection. (I) Cytograms demonstrating CD4+ T cell responsiveness to AT-2-inactivated SIVmac239, in an animal with 0.138% of cells producing both IFN-γ and TNF-α. The left cytogram is the result of stimulation with control microvesicles; the right cytogram is the result of stimulation with AT-2-inactivated SIVmac239.

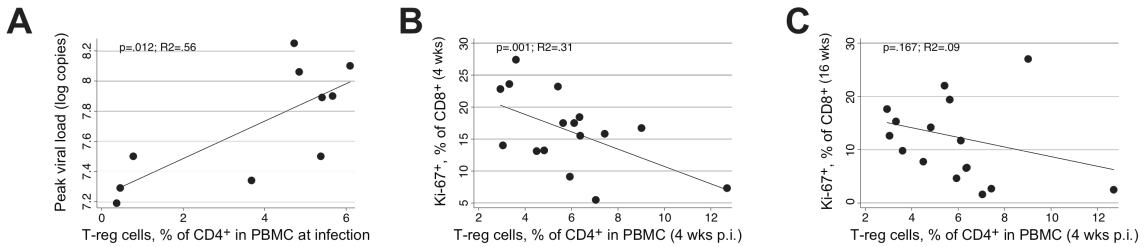

Figure S5. Relationship of T-regs to viral load and T cell activation.
(A) Among IL-2 and/or G-CSF-treated animals, T-regs present at infection are directly correlated with the peak viral load attained later. (B) Association between higher T-reg levels and lower generalized T cell activation (assessed here by Ki-67 expression in CD8+ T cells) at four weeks after infection. (C) Presence of more T-regs and lower T cell activation at earlier time points (as in B) did not translate into lower T cell activation at later time points (here, 16 weeks).

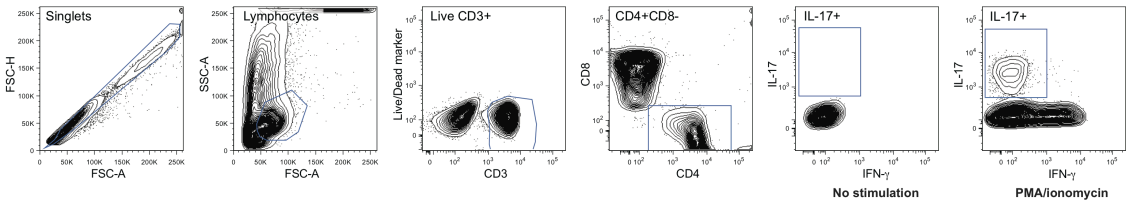

Figure S6. Gating tree and typical raw data for the IL-17 and IFN-γ parameters.
Gating tree for identification of IL-17-producing cells in unstimulated or PMA/ionomycin-stimulated samples.

Table S1. MHC alleles of animals in the observational study.

Identification in Fig. 2E	A01	B01	B08	B17	MHC Score
A	-	+	-	-	-1
B	-	+	-	-	-1
C	-	+	-	-	-1
D	-	-	-	-	0
E	-	-	-	-	0
F	-	-	-	-	0
G	-	-	+	-	1
H	-	-	-	+	1
I	-	-	+	-	1
J	+	-	-	-	1
K	+	-	+	-	2
L	+	-	-	+	2

MHC alleles of animals in the observational study. The MHC score was calculated by adding one point for each protective allele (Mamu-A*01, -B*08, and/or -B*17; see refs. 21, 31, 43, and 44) and subtracting a point for Mamu-B*01, which has been associated with higher viral loads (*21, 43*).